

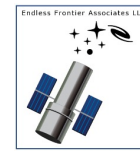
Integrated Modeling of a Segmented- Telescope Habitable Worlds Observatory

Structural, Control, and Optical Key Findings and Derived Design Guidance

AUGUST 10, 2023

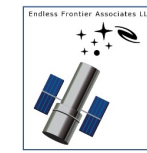
ALAIN CARRIER, LARRY DEWELL, MICHAEL JACOBY, KIARASH TAJDARAN

Outline

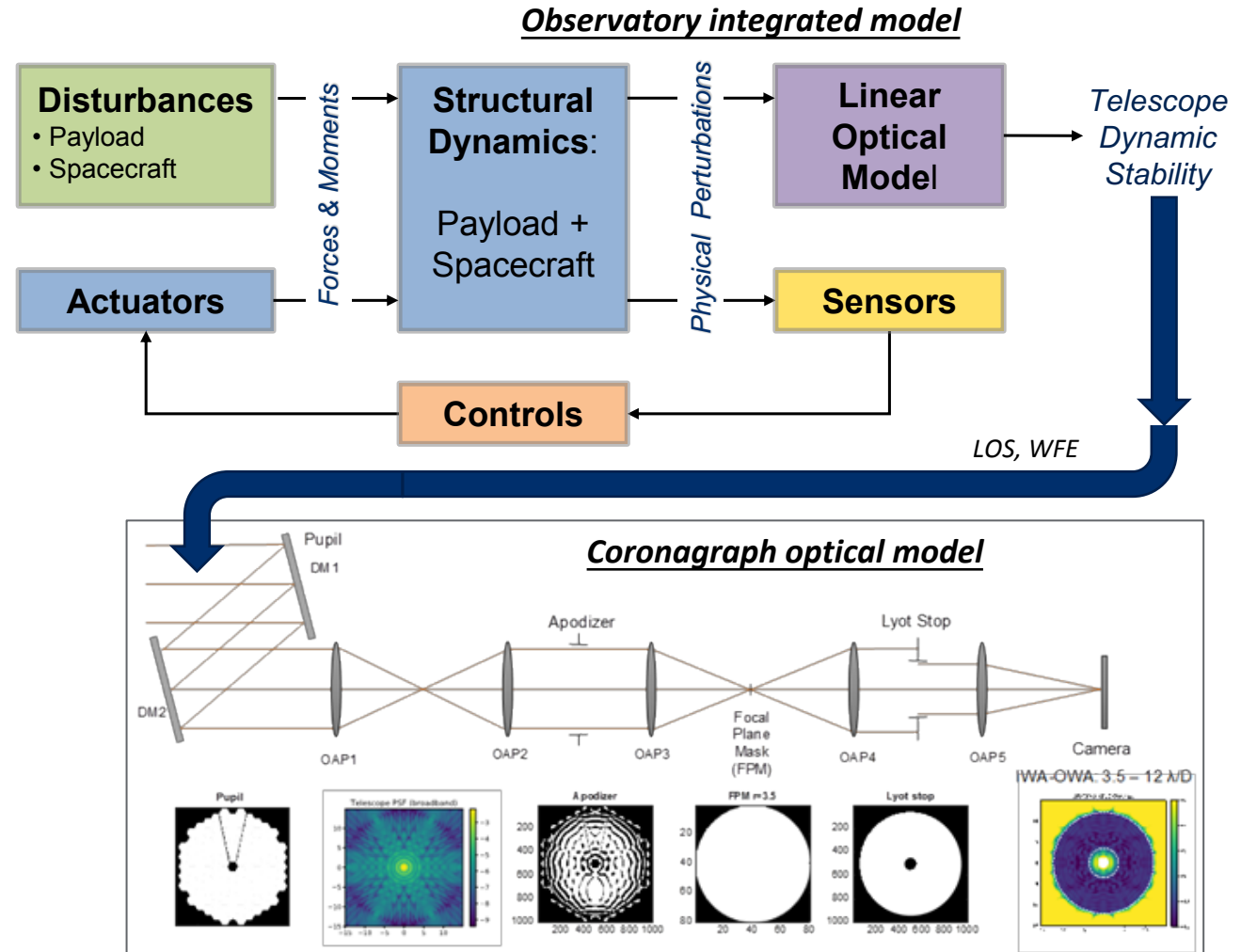


- **Motivations**
- **Summary integrated modeling infrastructure**
- **LUVOIR-B use-case**
- **Point design bottoms-up performance predictions**
- **Design Guidance for VIPPS-Enabled HWO Dynamic Stability**
- **Dynamic line-of-sight and wavefront error bottoms-up error budgets**
- **Discussion: Control-Structure Interaction Driven Segment-Alignment Control Bandwidth Limitation**

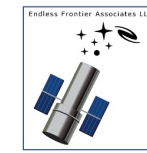
Motivation: Modeling to map observatory design to coronagraph contrast performance



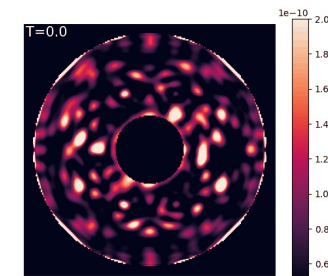
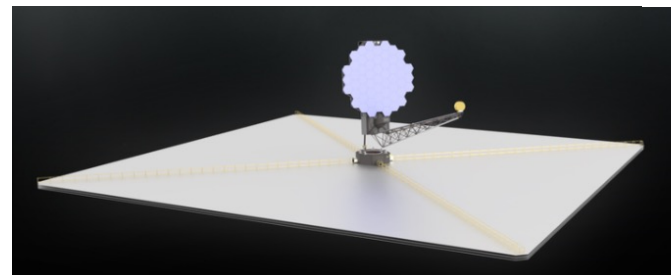
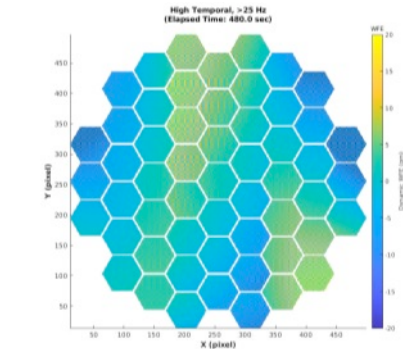
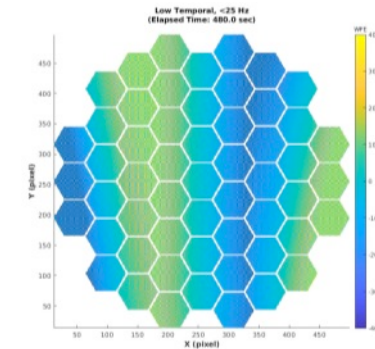
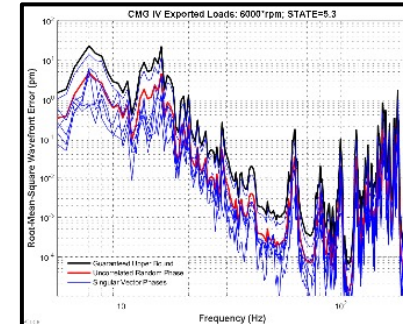
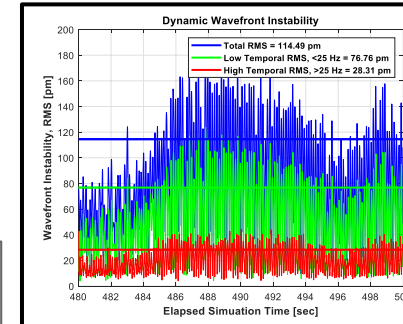
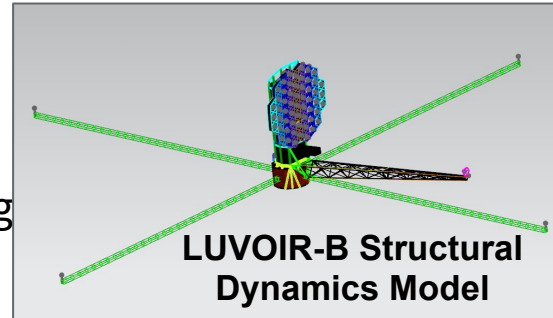
- Coronagraph instrument science yield and sensitivity is dependent on a stable LOS to target star and wavefront over long integration times
- The Habitable Worlds Observatory (HWO) will involve multiple interacting systems for controlling opto-mechanical stability, and will be impossible to test on the ground at system level
- Tightly coupled interdependencies require system-level evaluation of design alternatives and component sizing
- NASA and Industry Partners require powerful, rigorous and multi-disciplinary integrated modeling tools to enable model-based design early, and support observatory software development and system-level verification



Summary Integrated Modeling Capabilities

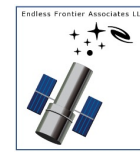


- Combined structural, control, and geometric optics
- System analyses in time and frequency domain
 - Matlab/Simulink-based; Model structured to facilitate linearization
- Structural model reduction
 - Anchored in line-of-sight and wavefront error metrics
- Non-contact Vibration Isolation & Precision Pointing System (VIPPS) performance predictions
 - Parametric representation facilitates trades/sizing
- Slew and settle analyses
 - Flexible body dynamics in large rotation
- Payload line-of-sight stability and dynamic wavefront error bottoms up performance predictions
- Derived design guidance and sensitivity studies
- Support for Coronagraph Technology Roadmap top-down yield analysis

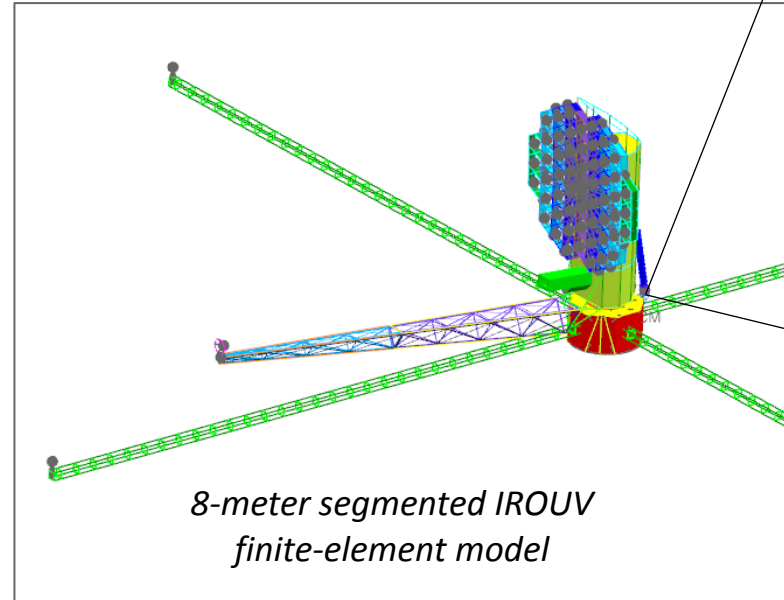


Dynamics Response (LM) → Contrast (Axel Potier SCDA)

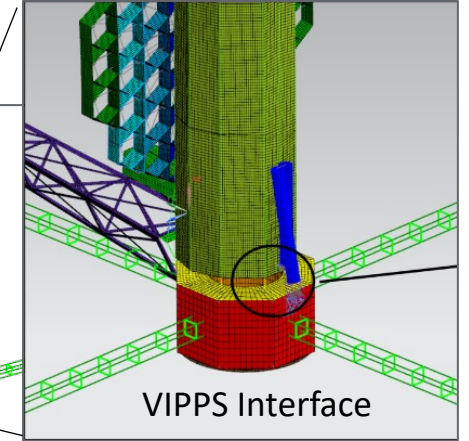
Use Case: Segmented telescope with VIPPS Interface, With Path to Multiple-Architecture Analysis of Alternatives



- Early IROUV architecture concepts described in Astro 2020 Decadal include diverse architectures
 - Segmented versus monolithic Primary Mirror
 - External occulter versus internal coronagraph instrument
 - Observatory torque actuation via micro-thrusters versus Control Moment Gyros (CMGs)
- LM-led TechMAST team focused on performance prediction of 8-meter segmented telescope with non-contact Vibration Isolation and Precision Pointing System (VIPPS)
 - Leverages LM prior development in Disturbance Free Payload (DFP) non-contact observatory architecture
- However, modeling architecture and tools are applicable to multiple architecture to support future evaluations of alternatives



*8-meter segmented IROUV
finite-element model*

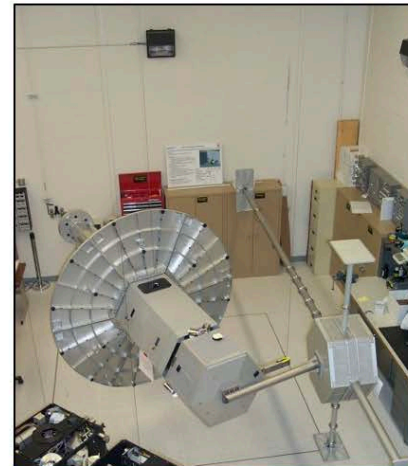
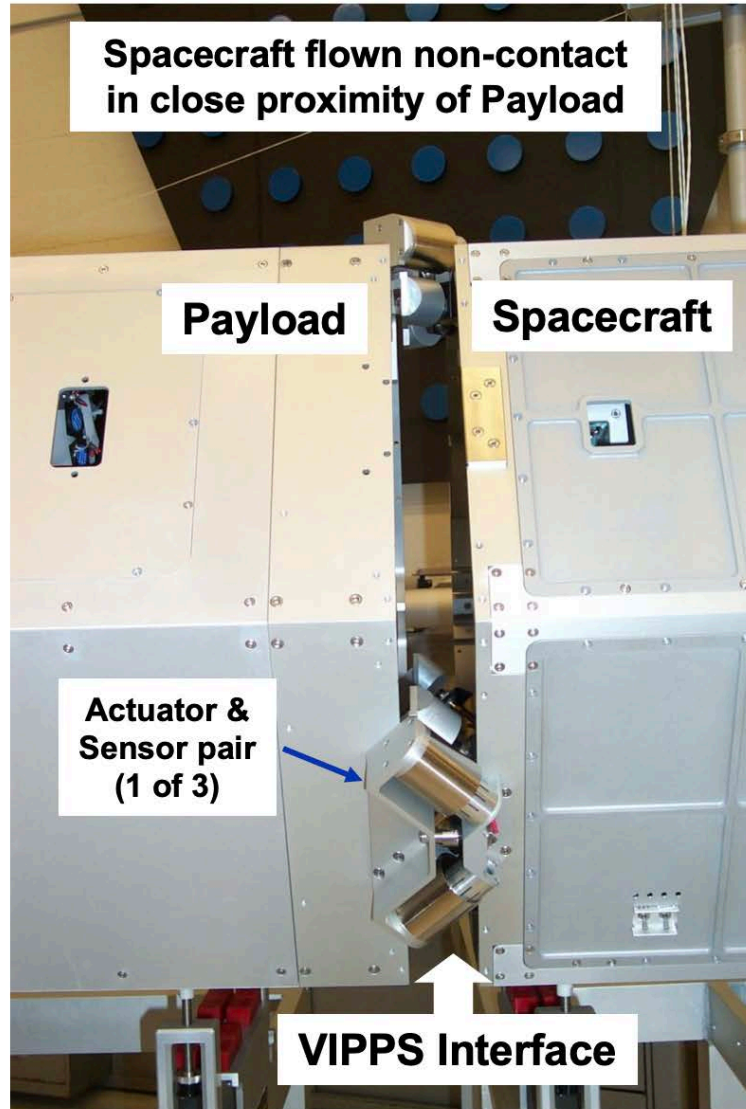
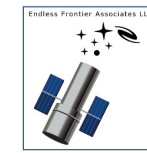


VIPPS Interface

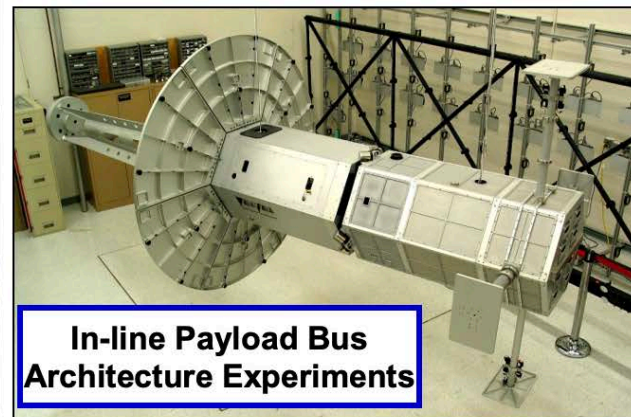


Lockheed Martin DFP testbed

Vibration Isolation & Precision Pointing System (VIPPS)



Demonstrated on Split Bus Architecture with Flexible Appendages

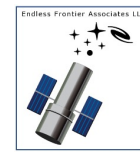


In-line Payload Bus Architecture Experiments

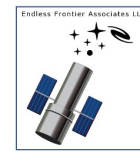
- **Architecture for Payload precision pointing and vibration isolation from host spacecraft**
 - Spacecraft follows Payload
- **Based on simple high-TRL components**
 - **Non-contact inductive position sensors**
 - Sensors provide information on relative pose between spacecraft and payload for spacecraft attitude and position control
 - **Large gap non-contact voice-coil actuators**
 - Actuators provide means to point Payload by reacting force on spacecraft based on Payload pointing sensor information or instructions without compromising vibration isolation
- **Variations on architecture for pointing only-VIPPS instead of full 6-degree-of-freedom VIPPS**

Summary of Integrated Modeling

Key Findings: Point Design and Bottoms-Up Performance



Finding	Description
Dynamic LOS stability bottoms-up prediction	LOS dynamic stability of 203 micro-arcsec (1σ , per-axis) against a self-imposed 300 micro-arcsec Threshold performance level.
LOS dynamic stability key contributors	Payload LOS error measurements derived from a High-Definition Imager (HDI) stare imaging are expected to be a dominant contributor to LOS stability. Detailed modeling of this measurement and estimation system is future integrated modeling effort
Dynamic WFE stability bottoms-up prediction	Dynamic Wavefront Error stability of 48.7 picometers (1σ) factors components state-of-the-art for specified use case. Predicted WFE divides between 45.6 and 16.8 pm of low- and high-spatial frequency error, respectively.
WFE dynamic stability key contributors	CMG exported disturbances and non-contact actuator current drive noise are expected to be the largest contributors to dynamic WFE stability performance. In addition, exported disturbances from telescope active alignment control is anticipated to be a contributor, but modeling of this effect is future integrated modeling work
Integrated modeling maturation in support of dynamic stability risk reduction	Additional modeling fidelity build-up, sensitivity studies and design analysis-of-alternatives are identified, in areas such as VIPPS interface cable coupling, interface placement in observatory, active alignment control system integration, and coronagraph contrast model integration, to name a few. Complete list provided in final report.

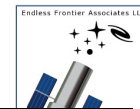


Summary of Integrated Modeling Key Findings: Design Guidance for VIPPS-Enabled HWO Dynamic Stability

- Analysis of the integrated observatory structure, VIPPS rigid-body control, Fine Steering Mirror (FSM) LOS control, and optical sensitivities resulted in significant insights into important areas to focus design, and key trades to execute
 - Design guidance summarized in final report
- Some significant design guidance findings are summarized in the table below

Key Design Guidance Area	Summary Description
VIPPS interface placement	This Study placed non-contact interface between instrument subassembly and multi-axis gimbal mechanism. Placement of VIPPS interface directly behind the telescope support structure could facilitate higher control bandwidth and reduced interface range of travel
VIPPS non-contact actuator drive noise	Drive noise is a significant contributor to WFE instability; minimizing its impact requires low-noise current sense amplifiers and linear drives. Trade exists between drive noise amplitude and observatory repointing agility
VIPPS interface cable stiffness	Minimize harness stiffness: incorporate wireless data/power transfer, and single-turn service loops for power
VIPPS Interface cable rate damping	Close knowledge gap on extent to which rate damping is present at frequencies 10x or more above coupled system resonance.
Fine Steering Mirror (FSM)	FSM-based LOS control is required for low-frequency disturbance rejection, and decouple VIPPS control bandwidth from settling time requirements; direct control from HDI LOS error measurement; passive reaction-cancelling design
Spacecraft Momentum Exchange Device Isolation	Passive isolation of momentum exchange devices (Honeywell M-160 CMGs considered in this study) are necessary; optimal WFE stability depends on proper placement of corner frequency and low isolation floor

Inertial Line-Of-Sight Instability Error Budget



Inertial Line-Of-Sight Instability: 300 usec (1 σ) Per Axis

		Error Source		Projected [usec (1 σ)]	Comments/Assmptions
1	VIPPS	Voice-Coil Actuators	Current Drive Noise	6	• One-sided noise spectral density: (1.0 uA/sqrt(Hz))/2.25
2			D/A Quantization	1	• Least-Significant Bit: (183 uA/bit)/16
3		Relative Position Sensors	Noise	1	• One-sided noise spectral density: 16.38 nm/sqrt(Hz)
4			A/D Quantization	2	• Least-Significant Bit: (0.366 um/bit)/8
5	Spacecraft	Momentum Exchange Devices (e.g. CMG)		13	• Honeywell M160 CMG IV: 6000 rpm • Vibration isolation system: 20-Hz natural frequency; Q=4
6		Fuel Slosh		50	• Allocation; >74-dB rejection below 1 Hz from VIPPS + FSM
7		Spacecraft Attitude Control System Jitter		50	• Allocation; >74-dB rejection below 1 Hz from VIPPS + FSM
8	Payload	Fine Steering Mirror	Actuator Current Drive Noise	69	• One-sided noise spectral density: 1.0 uA/sqrt(Hz) [6 N/Amp force constant]
9			Actuator Command Quantization	24	• Least-Significant Bit: 61 uA/bit
10			Relative Position Sensor	0	• Not used in steady-state observation: Feedback on HDI (no inner loop) • One-sided noise spectral density: 11.91 nrad/sqrt(Hz)
11		High Definition Imager Noise		145	• One-sided noise spectral density: 46 usec/sqrt(Hz) in object space (1/20 pixel resolution at 6.45 msec/pixel in visible) • Pointing data update rate: 100 Hz
12		Attitude Determination System		84	• Noise: 60 uarcsec (1 σ) DC to 0.1-Hz under steady-state pointing • VIPPS Payload inertial attitude control bandwidth: 36.5 mHz
13		Active Alignment Mechanisms		50	• Allocation • Mirror segment alignment system; Secondary Mirror alignment system
14		Margin		221	•
Total (Root-Sum-Squares)				300	

	Driver
	Not-Modeled

Dynamic Wavefront Error Budget



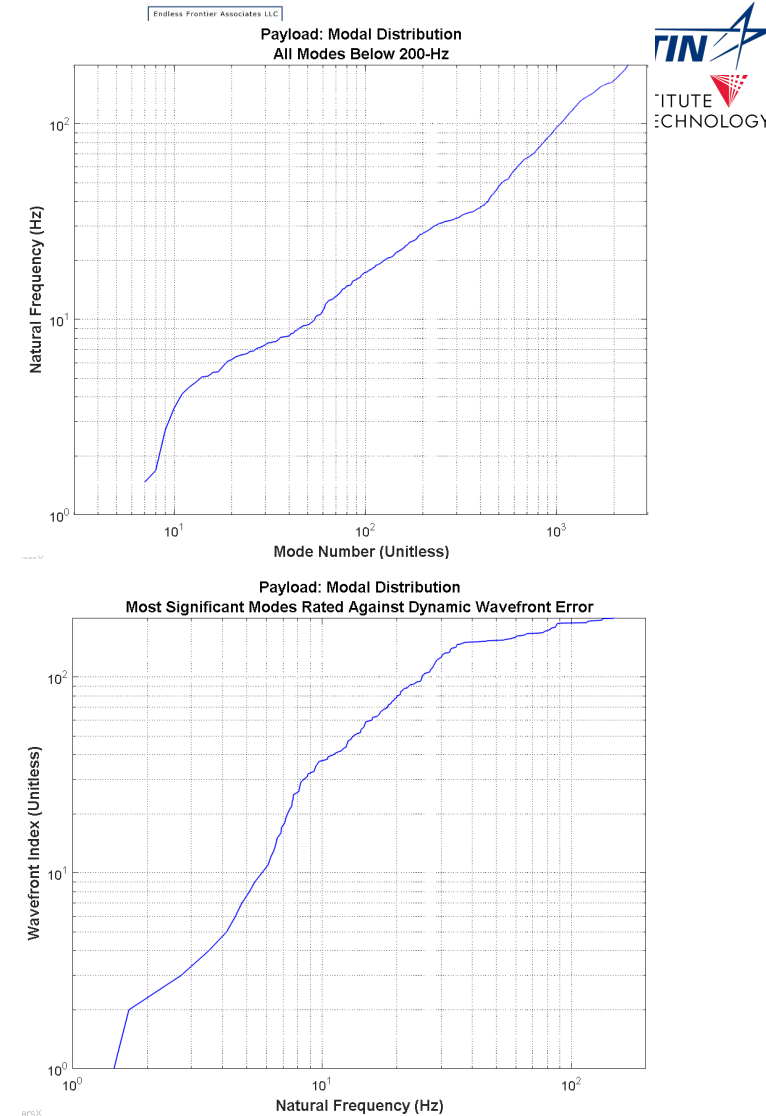
Dynamic Wavefront Error: Threshold: 50 pm (1 σ); Goal:10 pm (1 σ)

Error Source		Projected [pm (1 σ)]		Comments/Assmptions		
		<25 Hz	>25 Hz			
1	VIPPS	Voice-Coil Actuators	Current Drive Noise	34.1	12.6	• One-sided noise spectral density: (1.0 uA/sqrt(Hz))/2.25
2			D/A Quantization	4.3	1.6	• Least-Significant Bit: (183 uA/bit)/16
3		Relative Position Sensors	Noise	1.8	0.2	• One-sided noise spectral density: 16.38 nm/sqrt(Hz)
4			A/D Quantization	3.6	0.3	• Least-Significant Bit: (0.366 um/bit)/8
5	Spacecraft	Momentum Exchange Devices (e.g. CMG)		27.6	1.6	• Honeywell M160 CMG IV: 6000 rpm • Worst case phasing across excitation degrees-of-freedom • Vibration isolation system: 20-Hz natural frequency; Q=4
6		Fuel Slosh		1.0	1.0	• Allocation
7		Spacecraft Attitude Control System Jitter		1.0	1.0	• Allocation
8	Payload	Fine Steering Mirror	Actuator Current Drive Noise	4.1	3.2	• One-sided noise spectral density: 1.0 uA/sqrt(Hz) [6 N/Amp force constant]
9			Actuator Command Quantization	1.5	1.1	• Least-Significant Bit: 61 uA/bit
10			Relative Position Sensor Noise	0.0	0.0	• Not used in steady-state observation: Feedback on HDI (no inner loop) • One-sided noise spectral density: 11.91 nrad/sqrt(Hz)
11		High Definition Imager Noise		1.8	1.3	• One-sided noise spectral density: 46*uasec/sqrt(Hz) in object space • Pointing data update rate: 100 Hz
12	Attitude Determination System		1.0	1.0	• Allocation • Noise: 60 uarcsec (1 σ) DC to 0.1-Hz under steady-state pointing • VIPPS Payload inertial attitude control bandwidth: 36.5 mHz	
13	Active Alignment Mechanisms		10.0	10.0	• Allocation • Mirror segment alignment system; Secondary Mirror alignment system	
14	Margin		10.0	5.0	•	
Total (Root-Sum-Squares)			46.7	17.5	• Combined low & high: 49.9 pm (1 σ)	

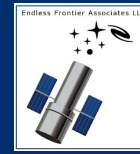
Driver
Not-Modeled

Segment-Alignment Control Bandwidth Limitation-- Control-Structure Interaction

- Segment alignment control system not yet part of integrated model
 - Major open task
- **Rule of thumb: segment alignment control bandwidth in segmented optical systems limited by control structure interaction to 1/5 to 1/10 of primary mirror assembly fundamental structure frequency**
 - Observation supported by experience on segmented ground telescopes and laboratory demonstrators
 - Fundamentally a control system stability matter, not an alignment performance regime matter
 - Large ratio of actuated mass (mirror segments) over reaction mass (support structure) drive extent of control-structure interaction
- **Top figure shows Payload modal distribution; Bottom figure counts number modes contributing most to wavefront error for LUVOIR-B point design**
 - Fundamental mode about 1.5 Hz; 48 flexible modes below 10 Hz
 - 10 modes below 6 Hz amongst major wavefront error contributors
- **Project segment-alignment control bandwidth on LUVOIR-B point design limited to less than 1 Hz: means totality of dynamics wavefront errors in prior error budget is in uncontrollable category**
 - Not within deformable mirror or segment alignment bandwidth

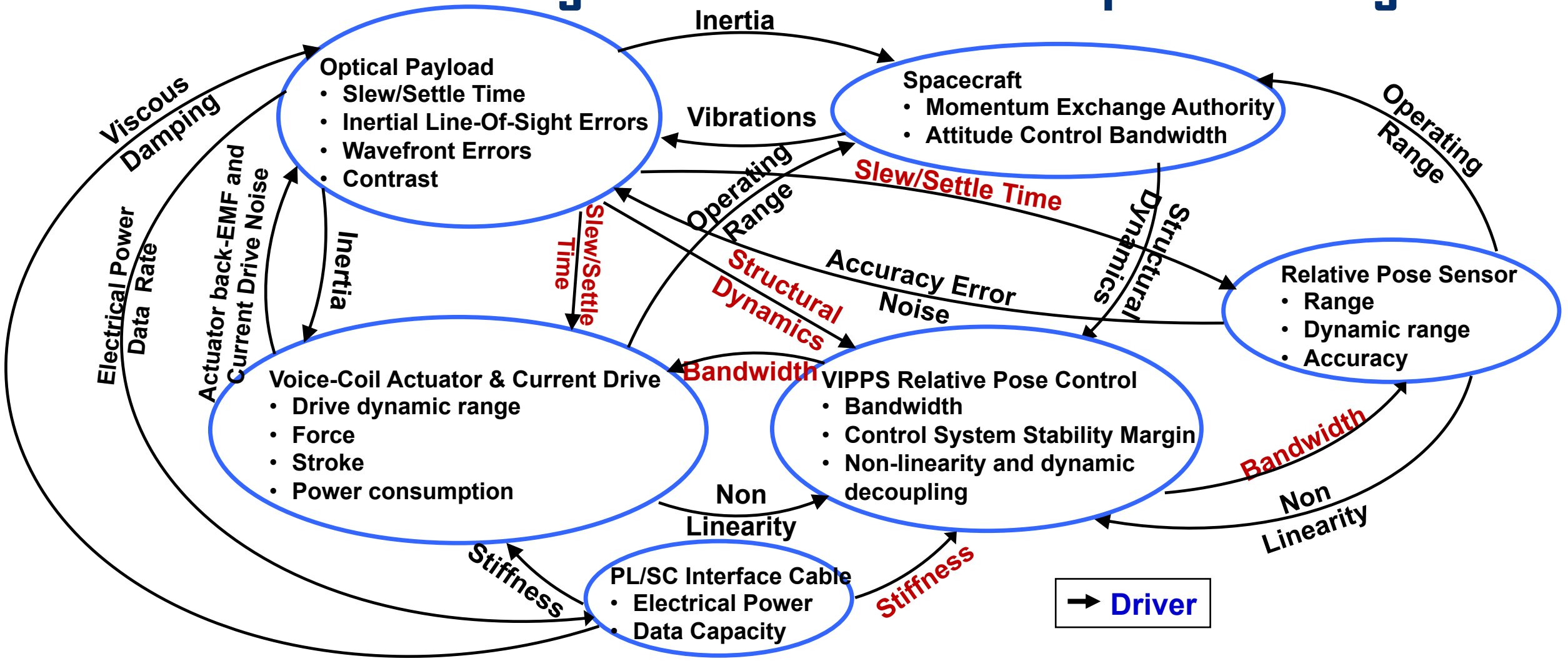
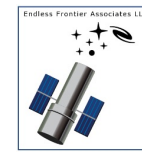


Challenge deserves attention: Architecture (e.g. stiffer primary mirror structure (>5 to 10 Hz), Segmented Fast Steering Mirror, etc...); Integrated modeling to inform design decisions

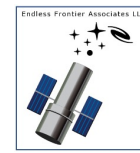


Backup

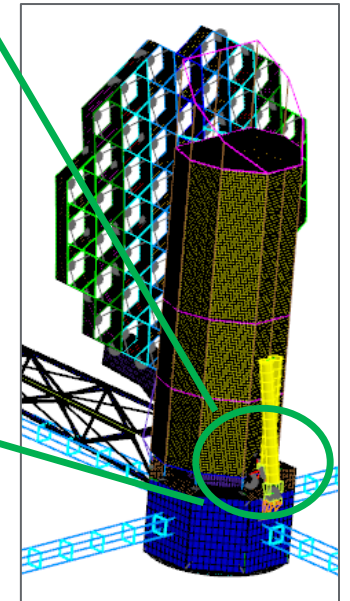
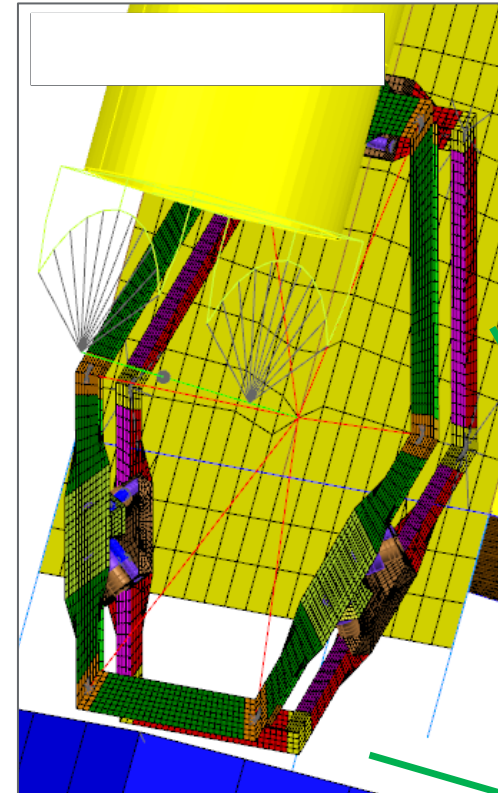
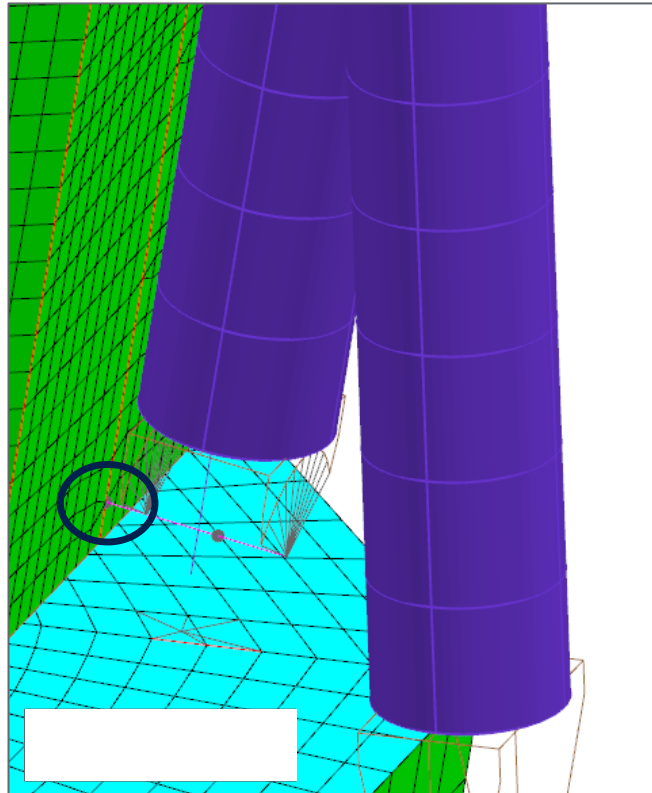
Tightly coupled interdependencies require system level evaluation of design alternatives and component sizing



Finite Element Model Upgrades

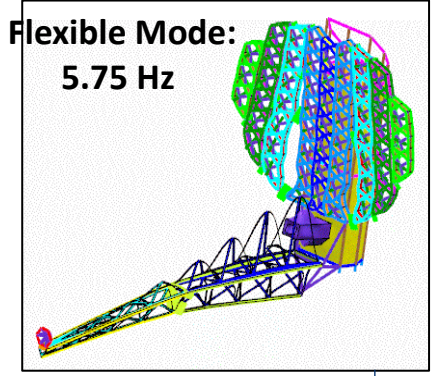
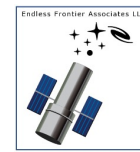


- IROUV model updated to include a representation of a distributed VIPPS interface (2022-2023 model)
 - Original model assumed an interface which was collapsed to two coincident nodes (2021 model)
- Model not intended to be an actual proposed interface design, but rather have features and behaviors that may be present in a realistic design, particularly
 - Local flexibilities within interface module
 - Non-collocated actuators and sensors
- All modeling to date assumes that during an observation, the articulation mechanisms & structure between payload and spacecraft are locked
- Typical high-TRL materials used
 - M55J/cyanate ester composites
 - Ti-6Al-4V fittings
- Section sizing based on engineering judgment and experience for now

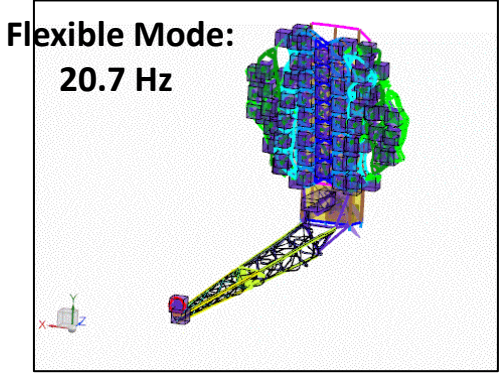
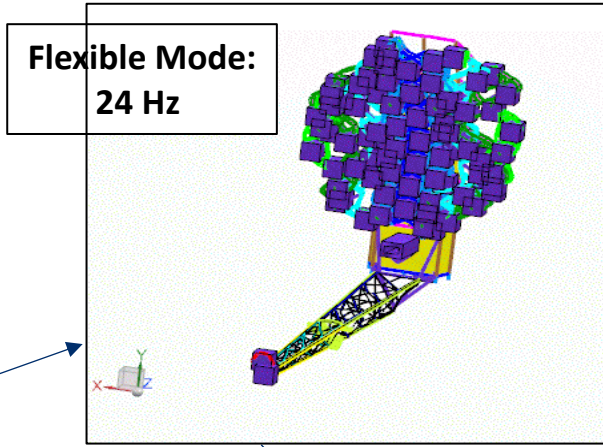


Non-Contact Interface model captures representative geometry, distributed structure, and standardizes conventions

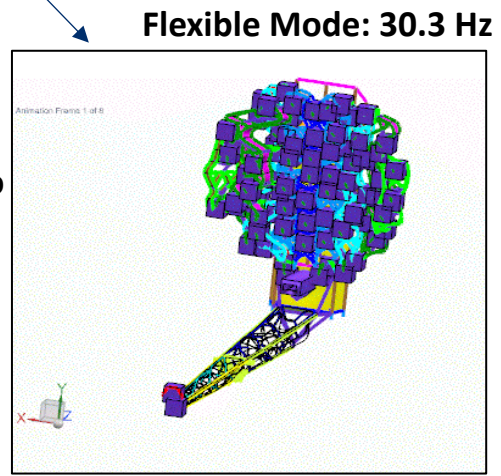
Dynamics: Transition from Low to High-Spatial Frequency Contribution



At low frequencies, PM mode shapes tend to be dominated by large-scale motion of the entire mirror, or large groupings of mirror segments, particularly along hinge lines

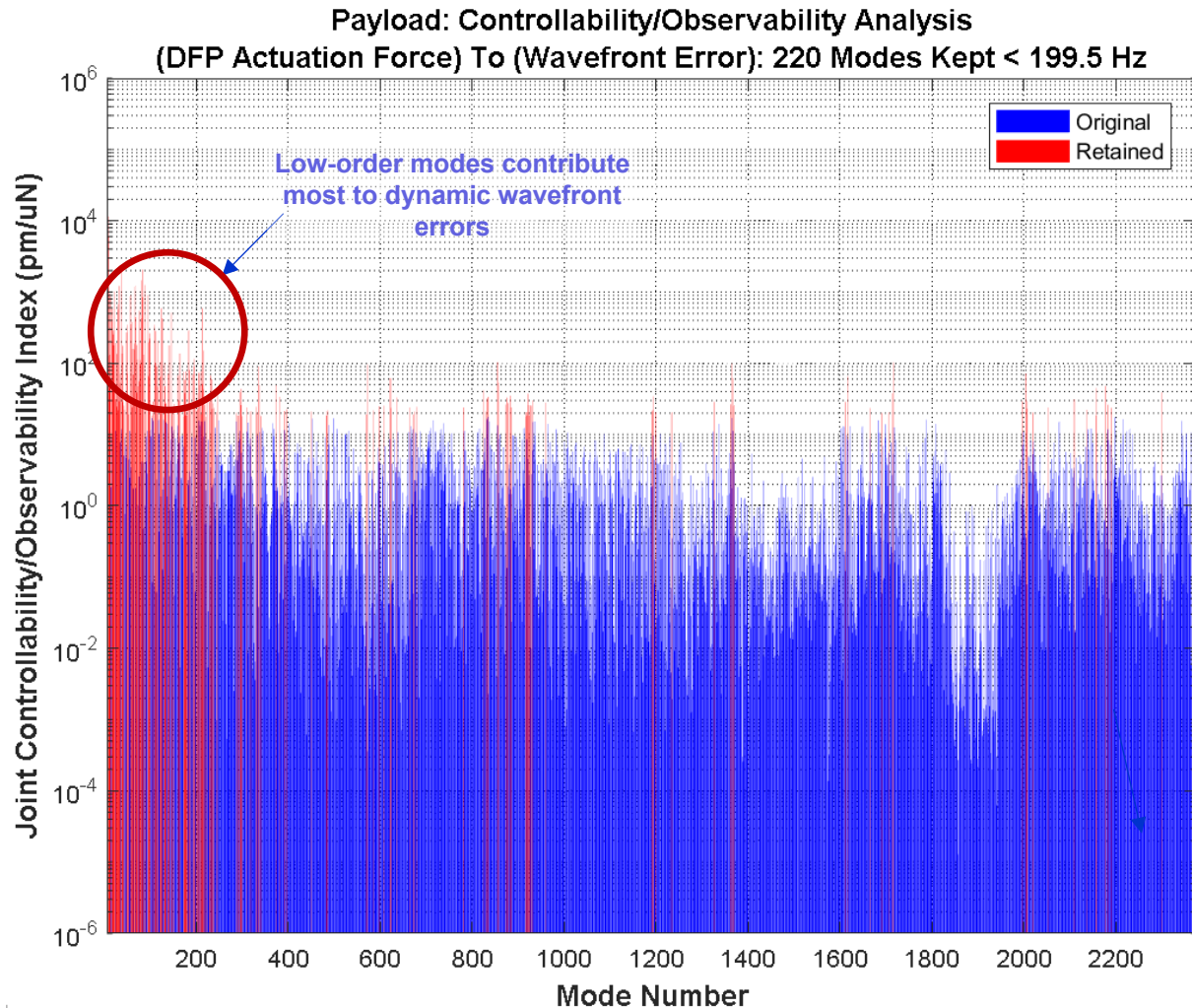
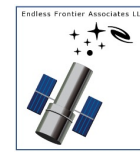


As the vibration frequencies approach ~25 Hz, the PM mode shapes transition from large groups of mirror segments to smaller numbers of mirror segments. The cubes at individual mirrors are added for clarity



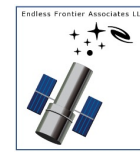
In Dynamics World, Transition From Low to High Spatial Frequency is Relatively High in Temporal Frequency: Visually About 25-Hz

Payload Structural Model Inspection From Dynamic Wavefront Error Perspective

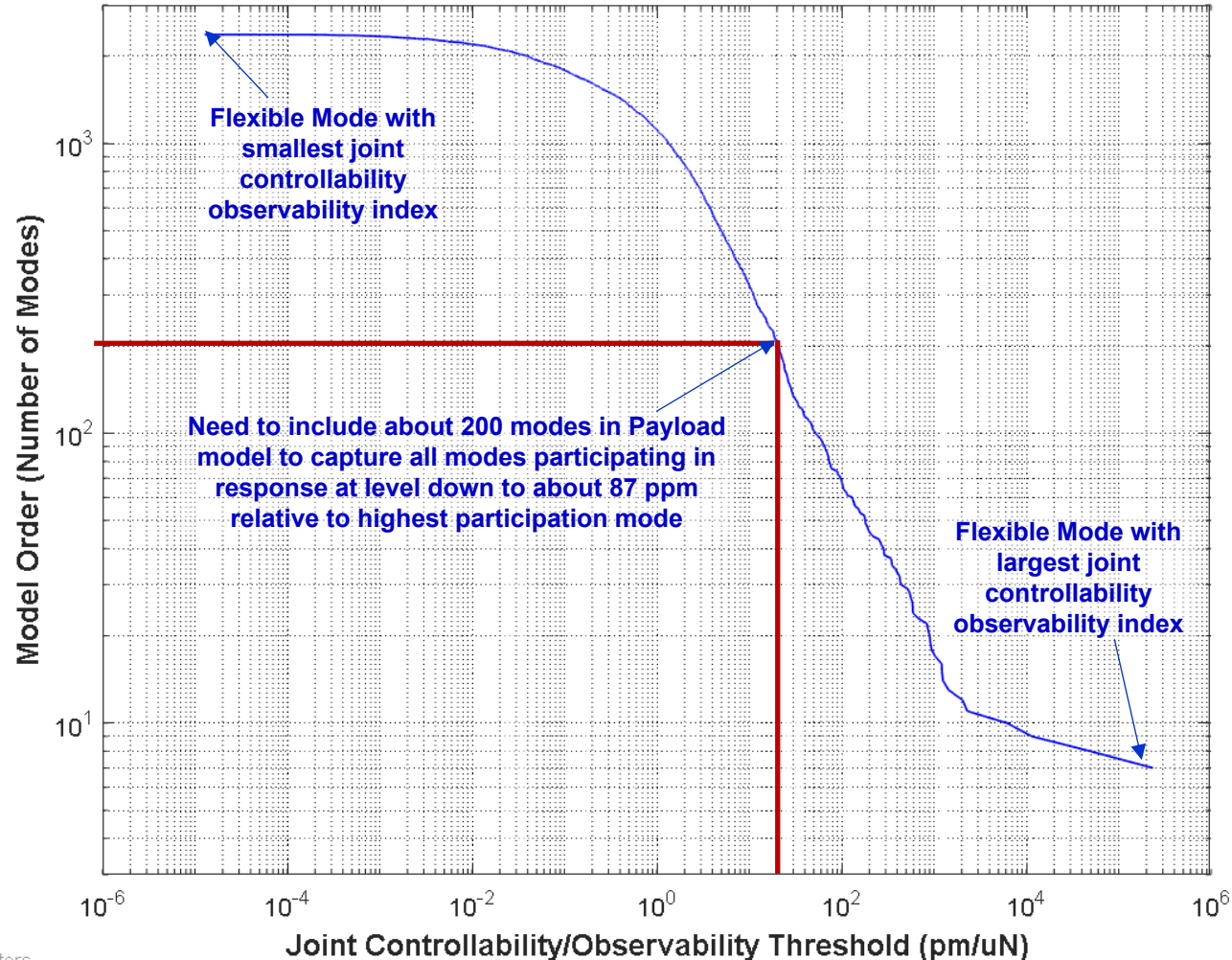


- **Analyzed payload structural modes contribution to dynamic wavefront errors from joint controllability/observability perspective using (VIPPS voice-coil actuator forces) as excitation source and (Payload dynamic wavefront error) as response**
 - Choice of actuation forces as source justified because VIPPS is only load path between spacecraft and payload
 - Controllability captures propensity for mode to being excited by loads applied to payload at VIPPS interface
 - Observability captures propensity for each mode to contribute to line-of-sight errors
 - Covers 2372 flexible modes with modal frequencies ranging from 1.468 Hz to 199.78 Hz; mode 1000 is near 95 Hz
- **Graphic shows payload modes joint controllability/observability versus payload mode number**
 - Modes are numbered in order of increasing natural frequency
 - First 220 modes contributing most to dynamic wavefront errors are highlighted in red (associated threshold is around 18 pm/uN or 13,000 times below dominant mode participation)

Payload Balanced Model Order Reduction From Dynamic Wavefront Error Perspective (1 of 2)



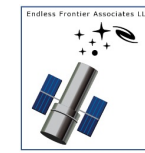
Payload: Controllability/Observability Analysis
Wavefront Error; Modal Distribution



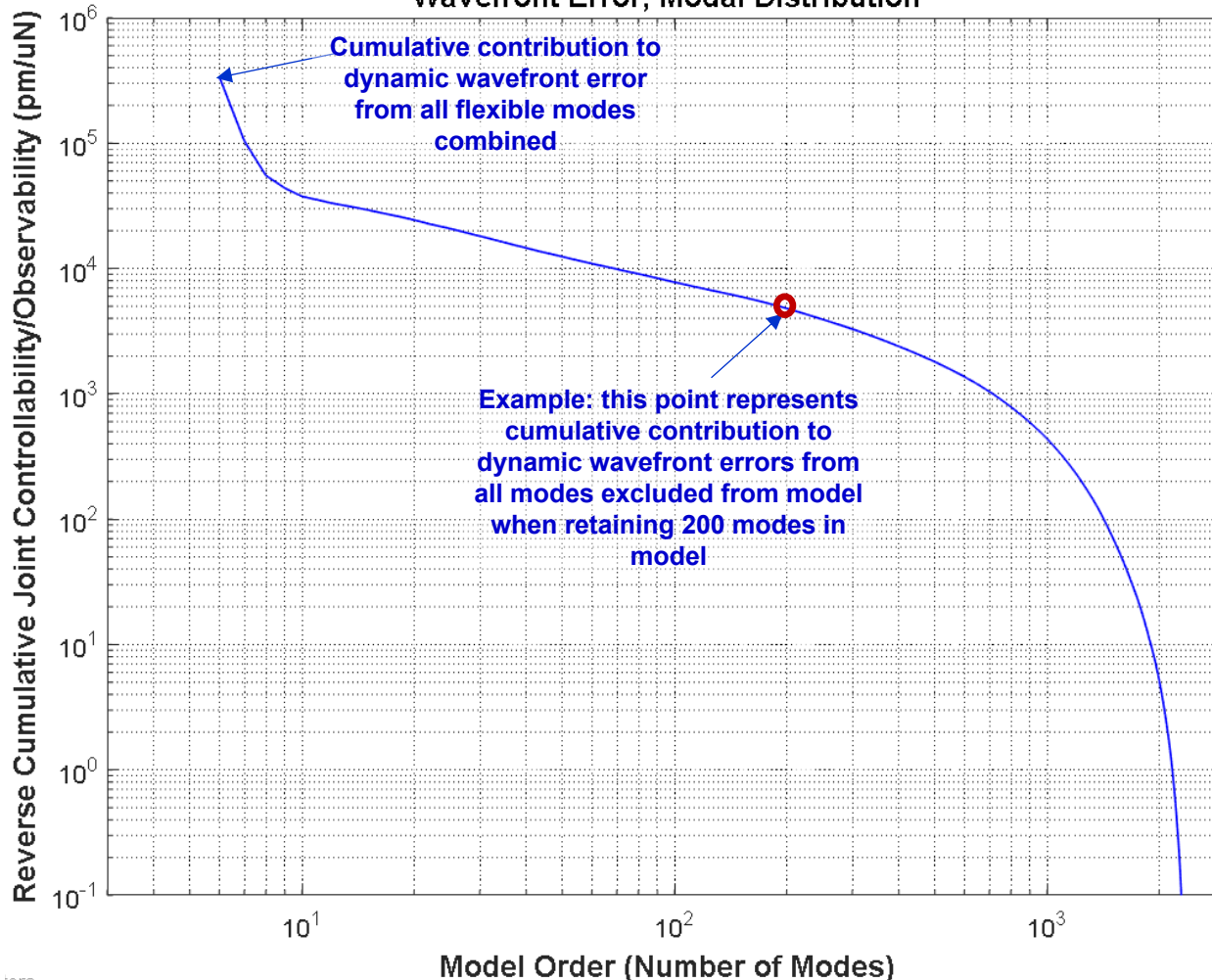
- **Ranked payload structural modes in terms of their joint controllability/observability index value from (VIPPS voice-coil actuator forces) to (Payload dynamic wavefront error) perspective**
 - Choice of actuation forces as input justified because VIPPS is only load path from spacecraft to payload
 - Controllability captures propensity for mode to be excited by loads applied to payload at VIPPS interface
 - Observability captures propensity for each mode to contribute to line-of-sight errors
- **Graphic shows payload model order versus joint controllability/observability threshold**
 - Payload reduced model order: about 200 modes when setting threshold at 10 pm/uN (captures all modes with contribution down to 87 ppm from that of mode contributing most to wavefront errors)

Joint Controllability/Observability Provides Quantitative Criterion For Ranking Importance of Each Payload Mode From Dynamic Wavefront Error Contribution Perspective

Payload Balanced Model Order Reduction From Dynamic Wavefront Error Perspective (2 of 2)

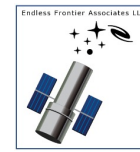


Payload: Controllability/Observability Analysis
Wavefront Error; Modal Distribution



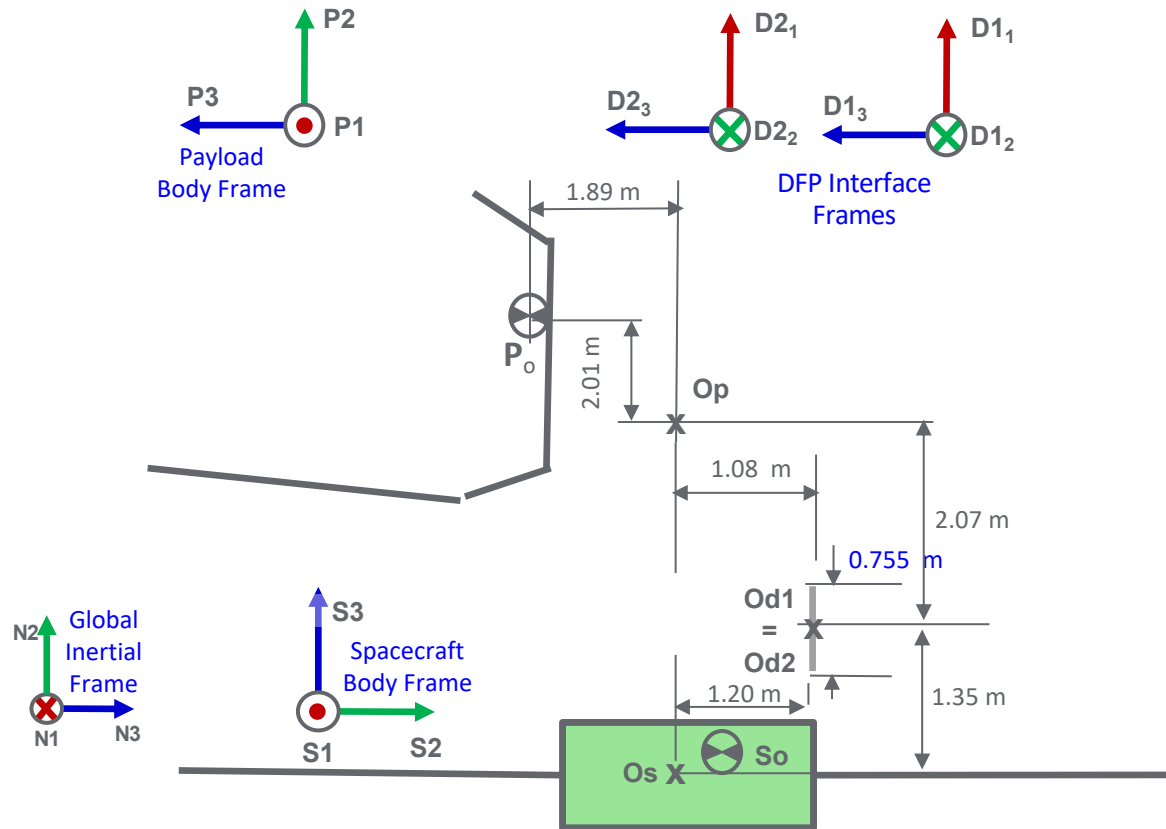
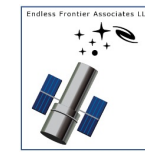
- **Cumulative contribution from many modes with dynamic wavefront error participation could still be significant**
 - Chart investigates that question
- **Graphic shows cumulative contribution to joint controllability/observability metric of all modes excluded from model versus model order**
 - Modes selected in descending joint controllability/observability index order
 - Including 220 modes in reduced order model would ensure 98.7% of dynamic wavefront errors are captured according to metric

Retaining 220 Modes in Payload Model Would Achieve Manageable Model Complexity While Capturing Dominant Portion of Dynamic Wavefront Errors



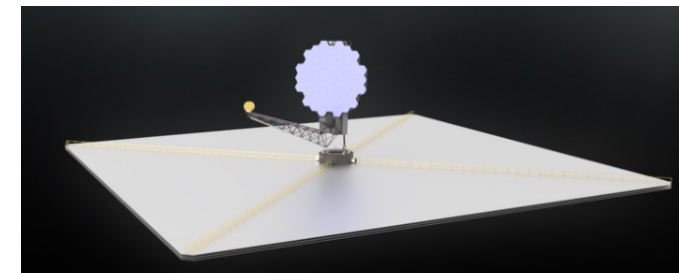
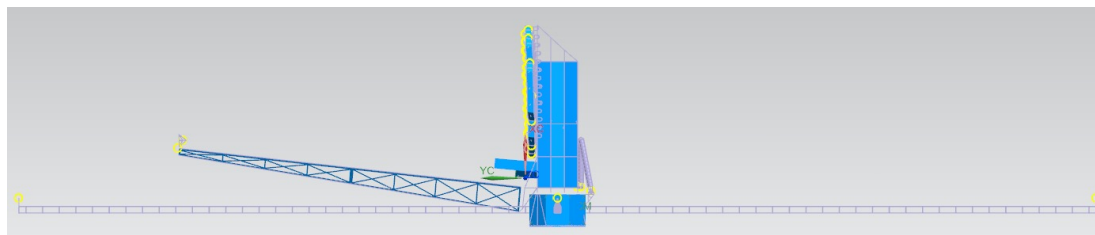
Design Departure Point

HWO Reference Coordinate Systems

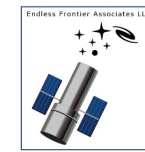


Physical Parameter	Value
Spacecraft bus mass	$M_b=7,518 \text{ kg}$
Bus center of mass location	$O_s B_o=(0.0082 \text{ m}) S_1 + (0.0759 \text{ m}) S_2 + (0.0603 \text{ m}) S_3$
Spacecraft bus central inertia dyadic resolved in "S"	$I_{Ib}=[\begin{matrix} 2.3271 & -0.0011 & -0.0008 \\ -0.0011 & 2.3160 & -0.0086 \\ -0.0008 & -0.0086 & 4.5634 \end{matrix}] * 1E5 * \text{kg} * \text{m}^2$
Spacecraft-To-DFP Interface location	$O_s O_{d1}=(0.000 \text{ m}) S_1 + (1.2045 \text{ m}) S_2 + (1.3528 * \text{m}) S_3$
Payload mass	$M_p=12,026 \text{ kg}$
Payload center of mass location	$O_p P_o=(0.2017 \text{ m}) P_1 + (2.0123 \text{ m}) P_2 + (1.8906 \text{ m}) P_3$
Payload central inertia dyadic resolved in "P"	$I_{I_p}=[\begin{matrix} 2.5280 & -0.0016 & -0.0003 \\ -0.0016 & 1.8958 & 0.2805 \\ -0.0003 & 0.2805 & 1.0408 \end{matrix}] * 1E5 * \text{kg} * \text{m}^2$
Payload-To-DFP Interface location	$O_p O_{d2}=(0.2081 \text{ m}) P_1 + (-2.0688 \text{ m}) P_2 + (-1.0784 \text{ m}) P_3$
DFP actuator mount radius	$R_a=37.8 \text{ cm}$
DFP voice-coil actuator stroke	$S_a=\pm 10 \text{ mm}$
DFP voice-coil actuator average force constant	$K_a=5 \text{ N/A}$

Ref: "data_transfer_v3_stiff-sc.mat" dated 01/13/2023



Design Departure Point (1 of 2)

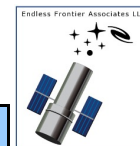


Habitable World Observatory: Spacecraft/Payload Non-Contact Design Baseline

Select Parameters		Value	Comments/Assmptions	
1	VIPPS	Actuator Mounting Radius	37.96 cm	
2		Non-Contract Voice-Coil Actuators	Stroke	+/-10 mm
3			Gap	12 mm
4			Force Constant	5.0-5.5 N/Amp
5			Peak Force	30 N
6			Continuous Force	15 N
7			Current Drive Peak Current	6.0 Amp
8			Current Drive Bandwidth	160 Hz
9			Current Drive Noise	1 uAmp/sqrt(Hz)
10			D/A Quantization	183 uAmp/bit
11	Non-Contact Relative Position		Range	+/-12 mm
12		Noise	16.38 nm/sqrt(Hz)	
13		A/D Quantization	366 nm/bit	
14		Bandwidth	30 kHz	
15	Control System	Digital Logic Update Rate	1 kHz	
16		Payload Inertial Attitude Control Bandwidth	36.5 mHz	
17		Spacecraft/Payload Relative Position Control Bandwidth	14 mHz	
18		Spacecraft/Payload Relative Attitude Control Bandwidth	3.8 mHz	
19		Spacecraft/Payload Relative Pose Estimator Bandwidth	0.2 Hz	
20		Gain Stabilization Quad Filter	0.1 to 0.3 Hz	

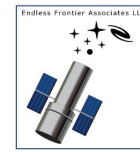
Driver

Design Departure Point (2 of 2)



Habitable World Observatory: Spacecraft/Payload Non-Contact Design Baseline						
		Select Parameters	Value	Comments/Assmptions		
1	Interface Cable	Coupled System Natural Frequency		0.4 to 1.1 mHz	• Based on Spacecraft and Payload rigid-body mass properties	
2		Effective Linear Stiffness		0.10 to 0.18 N/m	•	
3		Effective Rotational Stiffness		0.9 to 1.3 N*m/rad	•	
4		Viscous Damping Cut-Off Frequency		10*Fn	• Modeling means to acknowledge dominantly position-dependent (friction) nature of damping in cables • 10 x coupled system natural frequencies	
1	Spacecraft	Control Moment Gyroscopes	Number Of Units		4.00	• Single axis Honeywell M160 CMG IV: 6000 rpm nominal; Pyramid configuration
2			Peak Torque		87 N-m	• Each unit; Direct drive
3			Max Angular Momentum		200 N-m-sec	• Each unit
4			Vibration Isolation System		20 Hz; Q=4	• Natural frequency and amplification at resonance
5		Attitude Control Bandwidth		3.84 mHz	• Mode 1: Inertial attitude; Attitude Control System unused in Mode 3	
6		Fundamental Structural Natural Frequency		0.12 Hz	• Sunshield mode	
1	Payload	Fine Steering Mirror	Mirror Clear Aperture Diameter		23 cm	•
2			Tip/Tilt Control Bandwidth		50 Hz	• Inner loop on local relative position sensor: closed-loop -3 dB
3			Actuator Current Drive Noise		1 uA/sqrt(Hz)	• Actuator force constant 6 N/Amp
4			Actuator Command Quantization		61 uA/bit	• Least-Significant Bit; 16-bit D/A
5			Relative Position Sensor Noise		11.91 nrad/sqrt(Hz)	• Zeroed in steady-state observation to mimic feedback on HDI (no inner loop)
6			Line-Of-Sight Control Bandwidth		2.0 Hz	• Outer loop: 0-dB loop cross-over; Type-II logic
7		Fundamental Structural Natural Frequency		1.46 Hz	• Secondary mirror boom	
8		Compliance in load path from VIPPS interface to telescope		0.4 Hz	• First transmission zero	

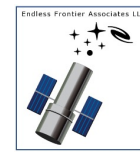
Driver



Spacecraft Vibration Transmissibility

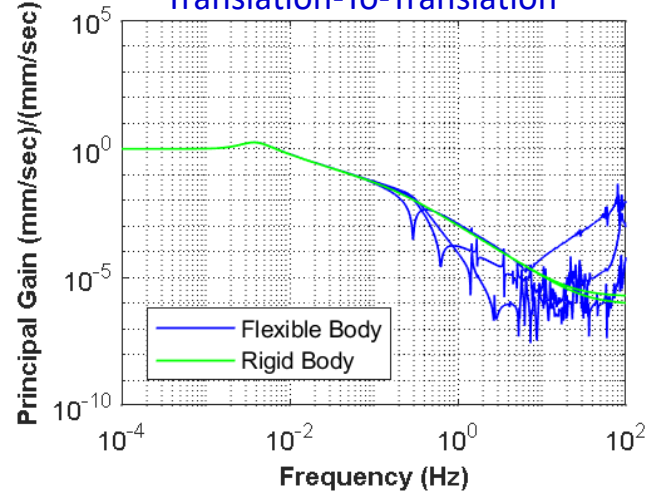
Spacecraft Vibration Transmissibility To Payload Inertial Pose

State: Pointing; Mode 3: Standalone; Actuator Current Drive Bandwidth: 160 Hz

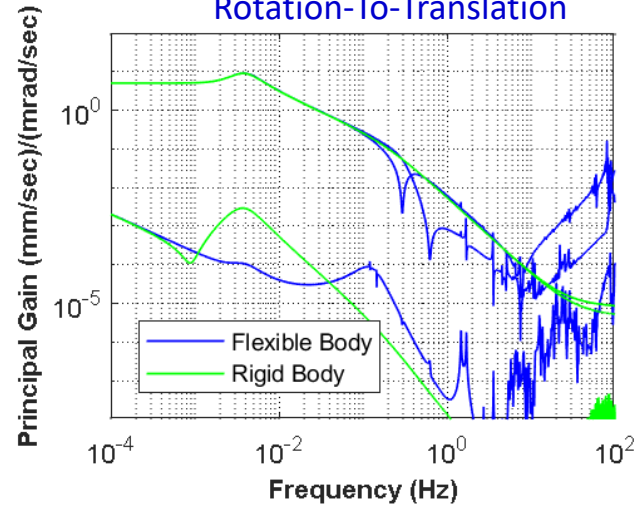


Transmissibility STATE=5.3: (Payload)/(Spacecraft)

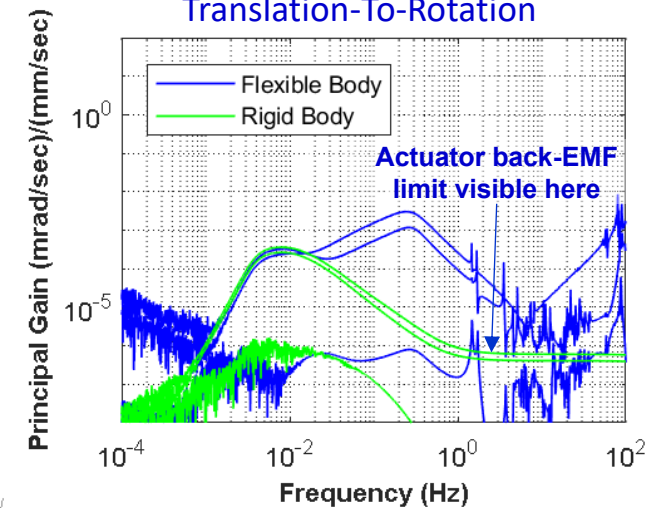
Translation-To-Translation



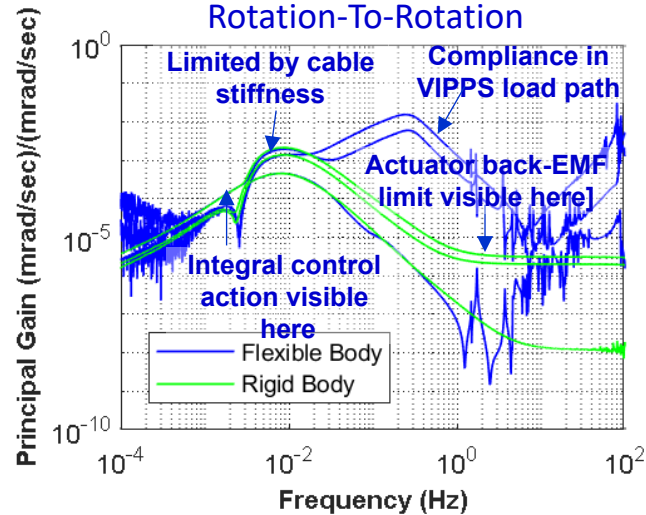
Rotation-To-Translation



Translation-To-Rotation



Rotation-To-Rotation



- **Graphic compares transmissibility from spacecraft vibrations to payload inertial pose referenced to payload center of mass in rigid-body and flexible-body cases from VIPSS vantage point**

- Control logic in standalone mode: VIPSS responsible for payload inertial pointing, relative position control, and spacecraft relative attitude control
 - Integral control enabled
 - Cable stiffness cancellation enabled
 - VIPSS uses spacecraft reaction-wheels as additional set of actuators
- Standalone control logic is fully decoupled at VIPSS interface

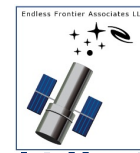
- **Transmissibility analysis shows**

- Decoupling from spacecraft inertial translation and rotation motion to payload inertial attitude
- Integral control logic and cable stiffness cancellation logic work as expected
- Rigid-body: attenuation limited by voice-coil actuator back-emf above 1 Hz and by cable stiffness below 1 Hz
- Deviation from rigid-body response dominated by compliance in VIPSS load path

Transmissibility dominated by compliance in VIPSS load path above 0.1 Hz

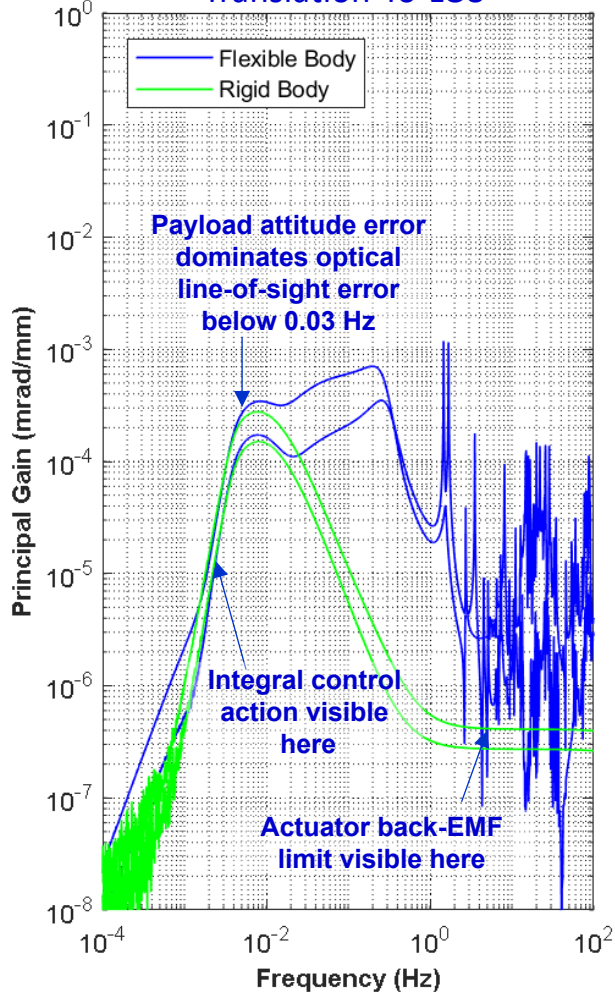
Spacecraft Vibration Transmissibility To Line-Of-Sight Error

State: Pointing; Mode 3: Standalone; Actuator Current Drive Bandwidth: 160 Hz; No Payload Line-Of-Sight Control

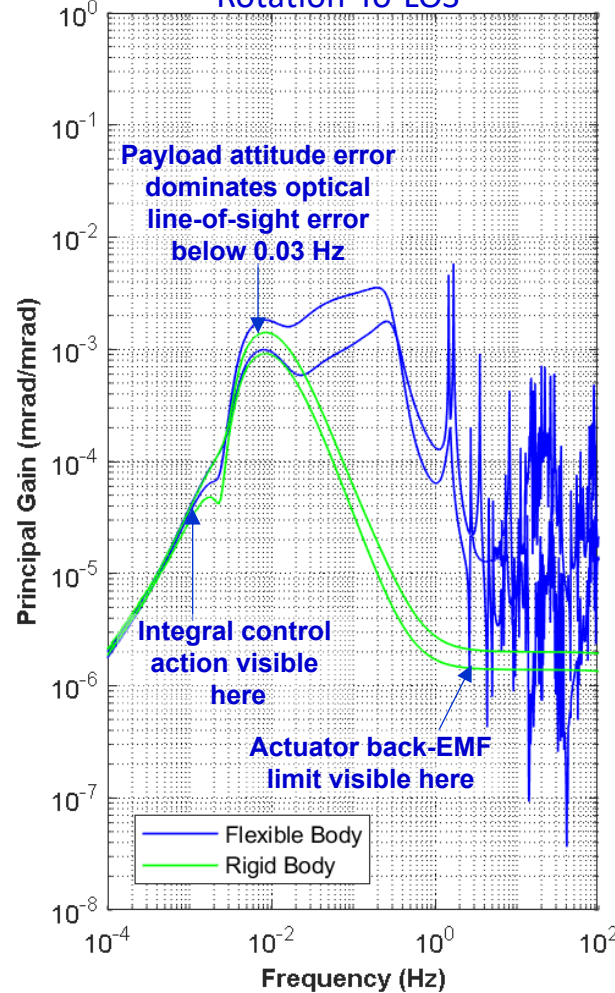


Transmissibility STATE=5.3: (Line-Of-Sight)/(Spacecraft)

Translation-To-LOS



Rotation-To-LOS



- **Graphic compares transmissibility from spacecraft vibrations to payload optical line-of-sight error in rigid-body and flexible-body cases**

- Control logic in standalone mode: VIPPS responsible for payload inertial pointing, relative position control, and spacecraft relative attitude control
- Integral control enabled
- Cable stiffness cancellation enabled
- DFP uses spacecraft reaction-wheels as additional set of actuators
- Standalone control logic is fully decoupled at VIPPS interface
- Payload Fine-Steering-Mirror-based line-of-sight control disabled

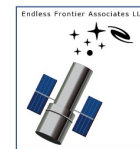
- **Transmissibility analysis shows**

- Payload attitude error dominates payload optical line-of-sight error below 0.03 Hz as expected (up to numerical accuracy)
- Rigid-body: performance limited by voice-coil actuator back-emf above 1 Hz and by cable stiffness below 1 Hz
- Flexible-body: transmissibility typically less than -49 dB except between 1 and 2 Hz; transmissibility less than -63 dB above 10 Hz

Typically Achieves 49 dB Vibration Disturbance Rejection in Absence Of Payload Attitude Sensing Errors

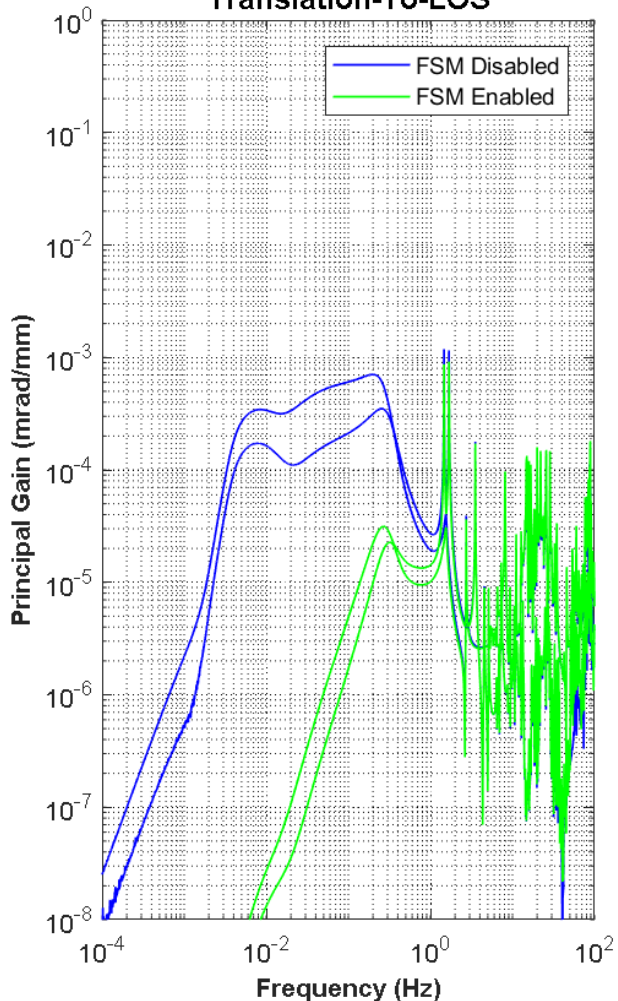
Spacecraft Vibration Transmissibility To Line-Of-Sight Error

State: Pointing; Mode 3: Standalone; Actuator Current Drive Bandwidth: 160 Hz; **Line-Of-Sight Control**

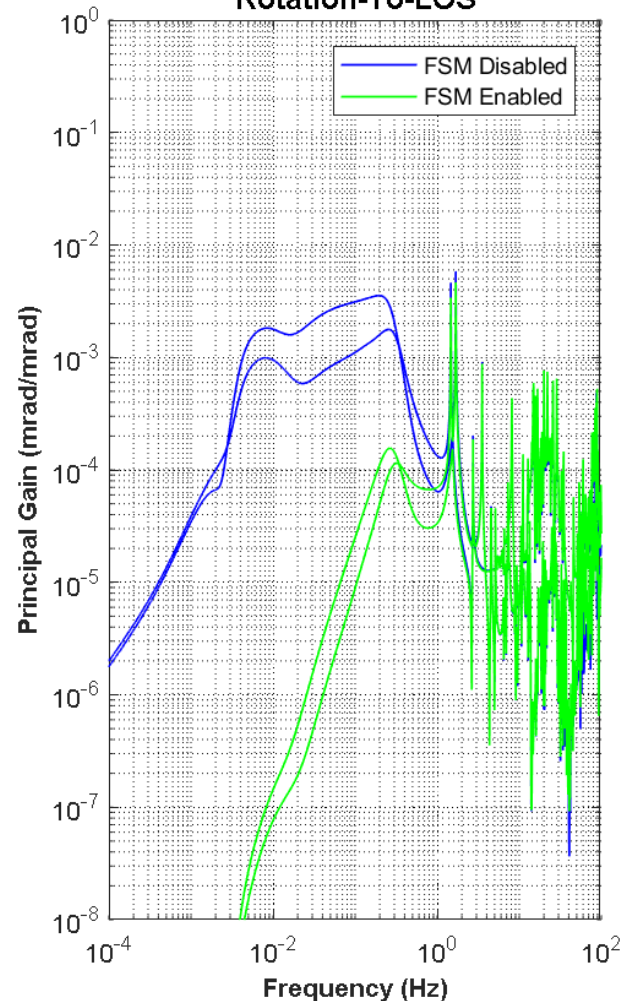


Transmissibility STATE=5.3: (Line-Of-Sight)/(Spacecraft)

Translation-To-LOS

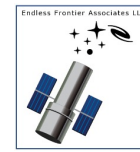


Rotation-To-LOS



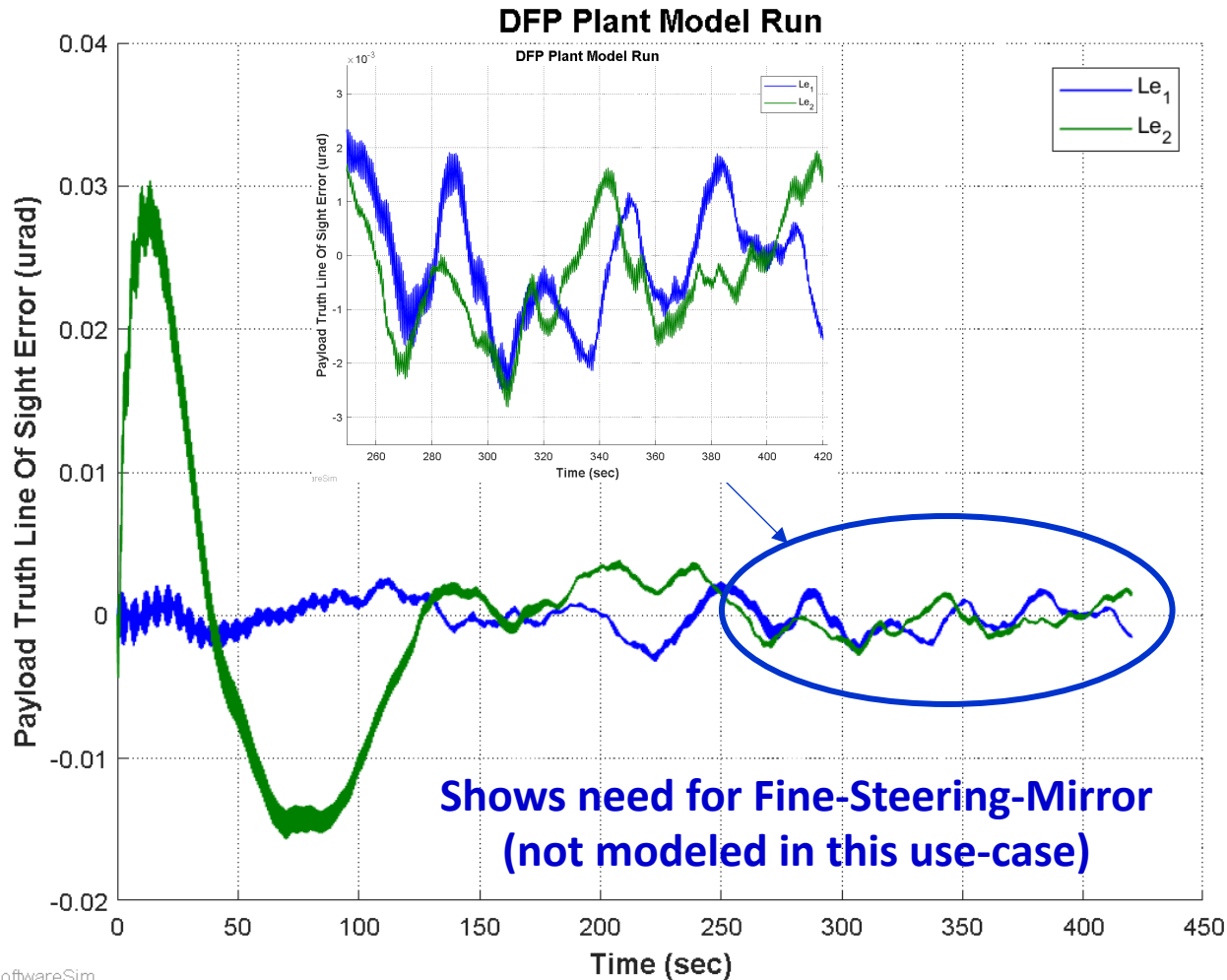
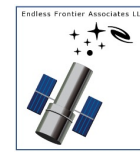
- **Graphic compares transmissibility from spacecraft vibrations to payload optical line-of-sight error with and without Payload inertial line-of-sight control enabled**
 - Control logic in standalone mode: VIPPS responsible for payload inertial pointing, relative position control, and spacecraft relative attitude control
 - Integral control enabled
 - Cable stiffness cancellation enabled
 - DFP uses spacecraft reaction-wheels as additional set of actuators
 - Standalone control logic is fully decoupled at VIPPS interface
- **Transmissibility analysis shows**
 - FSM Type-II outer loop control logic with 2-Hz 0-dB cross-over bandwidth provides about 40-dB residual disturbance rejection at 0.1 Hz
 - VIPPS and FSM in combination achieve 74 dB or more vibration disturbance rejection below 1 Hz
 - Transmissibility less than -63 dB above 4 Hz

Typically Achieves 63 dB Vibration Disturbance Rejection in Absence of Payload Attitude Sensing Errors



Transient Response

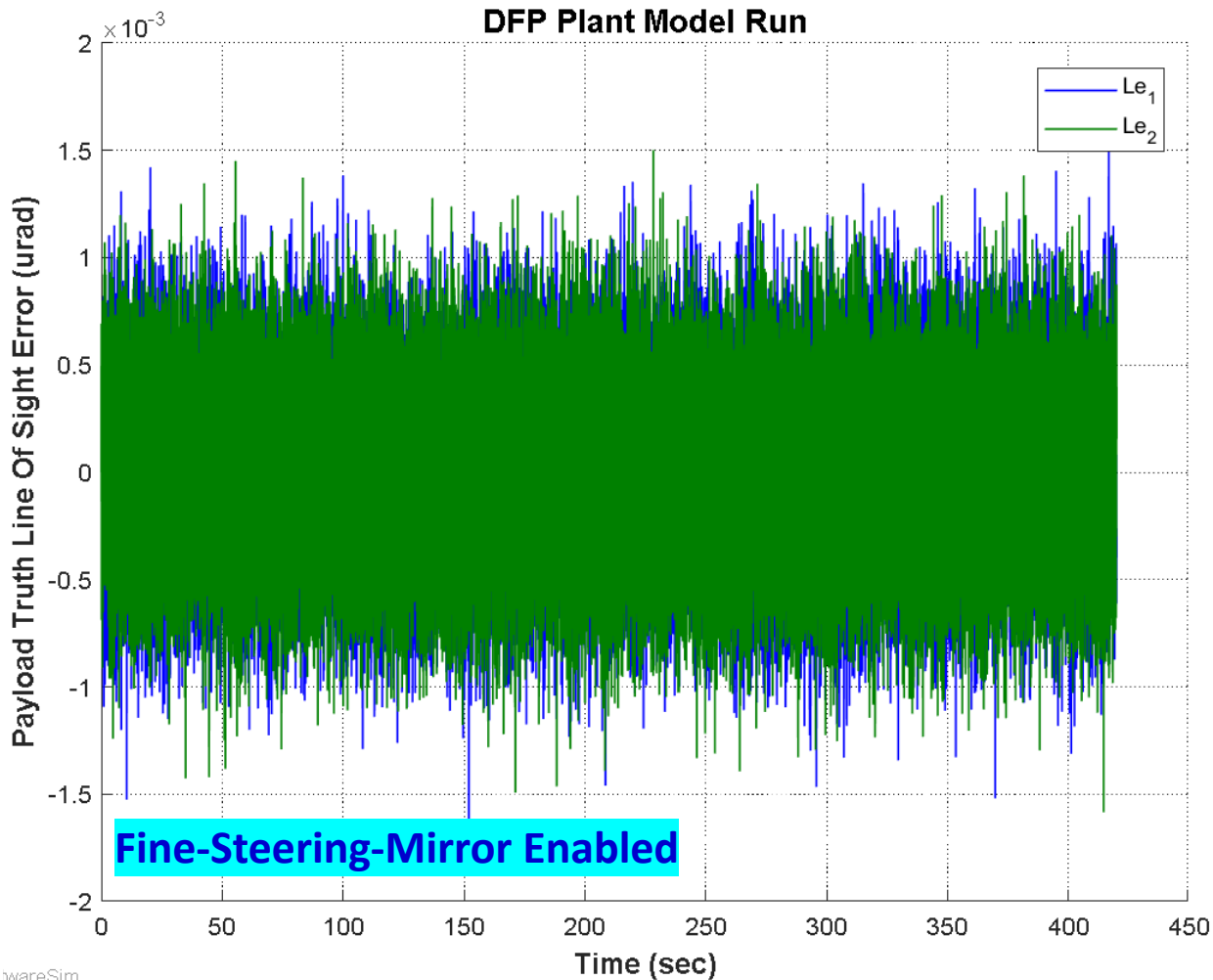
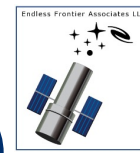
Example Transient Response: Impact of VIPPS Actuation and Relative Position Sensing Noise on Optical Line-Of-Sight (1 of 2)



- **Graphic shows optical line-of-sight error during small recentering activity at VIPPS interface**
 - Control logic in standalone mode: VIPPS responsible for payload inertial pointing, relative position control, and spacecraft relative attitude control
 - Random initial relative pose error between spacecraft and payload
 - Relative position: [0.9964; -0.0024; 0.1474] mm
 - Relative attitude: [0.0 0.0 0.0] deg
 - Actuator linear drive current noise: 1 uA/sqrt(Hz)
 - Actuator command D2A quantization: 183 uA/bit
 - Relative position sensor noise: 16.38 nm/sqrt(Hz)
 - Relative position sensor quantization: 0.3662 um/bit
- **Observed optical line-of-sight errors**
 - <2.8 nrad (577 usec) 0-peak after 250 sec
 - [1.07 1.10] nrad ([221; 228] usec) (1σ) after 250 sec
 - Modal excitation 72 usec 0-to-peak typical at 1.47 Hz

Optical Line-Of-Sight Errors in initial transient use-case dominated by low-frequency drift of [0.22; 0.23] msec (1σ) after 250 sec

Example Transient Response: Impact of VIPPS Actuation and Relative Position Sensing Noise on Optical Line-Of-Sight (2 of 2)



- **Graphic shows optical line-of-sight error during small recentering activity at VIPPS interface with FSM enabled**
 - Control logic in standalone mode: VIPPS responsible for payload inertial pointing, relative position control, and spacecraft relative attitude control
 - Random initial relative pose error between spacecraft and payload
 - Relative position: [0.5637; -0.1743; -0.4679] mm
 - Relative attitude: [0.0 0.0 0.0] deg
 - Actuator linear drive current noise: 1 $\mu\text{A}/\sqrt{\text{Hz}}$
 - Actuator command D2A quantization: 183 $\mu\text{A}/\text{bit}$
 - Relative position sensor noise: 16.38 $\text{nm}/\sqrt{\text{Hz}}$
 - Relative position sensor quantization: 366.2 nm/bit
 - Fine Steering Mirror actuator noise: 1.0 $\mu\text{A}/\sqrt{\text{Hz}}$
- **Observed optical line-of-sight errors**
 - [0.347 0.348] nrad ([71.5; 71.9] μsec) (1σ)

FSM reduces Optical Line-Of-Sight Errors in initial transient to less than 72 μsec (1σ)